

Abstract

Smith-Purcell radiation is emitted by an electron moving close to the periodically inhomogeneous target. The main features of Smith-Purcell radiation is monochromaticity and relation between the wavelength of radiation and the observation angle. As during generation there is no direct interaction of the electron with the material, this radiation can serve as a tool for non-invasive beam diagnostics. We report on the latest progress in theoretical investigation of Smith-Purcell radiation emitted by an electron from two-periodical arrays of small particles. Such targets are sometime referred as metasurfaces or photonic crystals. Second period in direction perpendicular to the electron trajectory opens new possibilities for diagnostics

1. Smith-Purcell Radiation

Smith-Purcell radiation (SPR) is emitted by a charge moving near a periodically inhomogeneous target. Purcell and Smith first measured it in 1953 and since then SPR has been studied for wide range of gratings and in different frequency ranges.

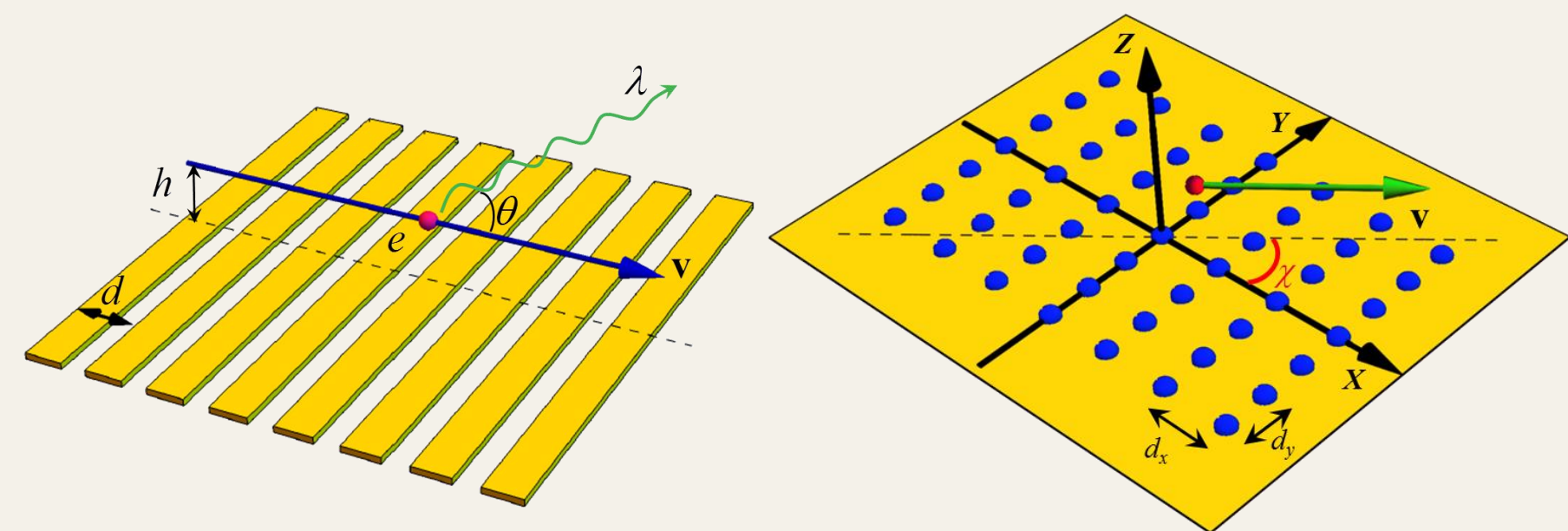


Fig. 1. Smith-Purcell radiation from usual grating

Fig. 2. Smith-Purcell radiation from an array of particles (Metasurface)

The main feature of SPR appears in dispersion relation. For the usual grating it has the form:

$$d(\beta^{-1} - \cos \theta) = s\lambda, s = 1, 2, \dots \quad (1)$$

Because of the second period there are two dispersion relations for SPR from a metasurface of sub-wavelength particles:

$$\lambda s_x = d_x \left(\frac{\beta_x}{\beta^2} - n_x \right), \quad (2)$$

$$\lambda s_y = d_y \left(\frac{\beta_y}{\beta^2} - n_y \right), \quad (3)$$

where λ is the wavelength of radiation; s_x and s_y are integers; d_x and d_y are the periods of the gratings; $\beta = v/c$, with v being the velocity of the electron, c being the speed of light; β_x and β_y are the corresponding components of the vector β ; n_x and n_y are the components of the unit wave vector.

2. Theory of SPR from an Array

The target is a finite number of identical small objects of radius $r_0 \ll \lambda$ that are located at the sites of a 2D rectangular lattice. The radius-vector of m -th particle is

$$\mathbf{R}_m = d_x m_x \mathbf{e}_x + d_y m_y \mathbf{e}_y, \quad (4)$$

$$m_x \in [-N, N], m_y \in [-M, M].$$

A free electron is travelling parallel to the target plane with velocity \mathbf{v} and impact parameter h , which is the shortest distance between the electron and the target. The projection of velocity on the plane OXY makes an angle χ with the x -axis, i.e. $\mathbf{v} = v(\cos \chi, \sin \chi, 0)$.

Solving microscopic Maxwell's equations and further expressing the field components through the charge e and the current densities of an electron we find the Fourier transform of the microscopic field:

$$\mathbf{E}^{\text{mic}}(\mathbf{r}, \omega) = -\frac{4\pi i}{\omega} \times \int d\mathbf{q} e^{i\mathbf{q}\cdot\mathbf{r}} \frac{\mathbf{q}(\mathbf{q}, \mathbf{j}^{\text{mic}}(\mathbf{q}, \omega)) - k^2 \mathbf{j}^{\text{mic}}(\mathbf{q}, \omega)}{q^2 - k^2}, \quad (5)$$

where the frequency ω , the velocity of light in vacuum c and the wave number k are related by $k = \omega/c$. The total current density \mathbf{j}^{mic} consists of the current density of the free electron \mathbf{j}^0 and the current density \mathbf{j} , induced in the target: $\mathbf{j}^{\text{mic}} = \mathbf{j}^0 + \mathbf{j}$. For the sub-wavelength particles the dipole approximation is applicable for calculation the current density:

$$\mathbf{j}(\mathbf{r}, \omega) = -i\omega \sum_m \mathbf{d}(\mathbf{R}_m, \omega) \delta(\mathbf{r} - \mathbf{R}_m), \quad (6)$$

where δ is the Dirac delta function, \mathbf{d} is the dipole moment that can be expressed through the polarizability of object's $\alpha(\omega)$:

$$\mathbf{d}(\mathbf{R}_m, \omega) = \alpha(\omega) \mathbf{E}^{\text{mic}}(\mathbf{R}_m, \omega). \quad (7)$$

The total field of radiation in the far zone ($kr \gg 1$) represents the field (5) excluding the Coulomb field of the moving electron.

3. Field of Radiation

The total field of Smith-Purcell radiation from a 2D array of small particles has the form:

$$\mathbf{E}(\mathbf{r}, \omega) \Big|_{kr \gg 1} = \alpha(\omega) \frac{e\omega}{\pi c^2 \beta^2 \gamma} \frac{e^{ikr}}{r} \times \sum_m e^{i\mathbf{d}_m \cdot \mathbf{k}} e^{i\mathbf{d}_m \cdot \mathbf{p}_m} [\mathbf{k}, [\mathbf{k}, \mathbf{P}_m]], \quad (8)$$

where k_x and k_y are the corresponding components of the wave vector $\mathbf{k} = k\mathbf{n}$, \mathbf{n} is the unit wave-vector,

$$\varphi_x = \frac{\omega v_x}{v^2} - k_x, \quad \varphi_y = \frac{\omega v_y}{v^2} - k_y, \quad (9)$$

$$\mathbf{P}_m = \frac{i}{\gamma v} K_0 \left(L_m \frac{\omega}{v\gamma} \right) + \frac{\mathbf{L}_m}{L_m} K_1 \left(L_m \frac{\omega}{v\gamma} \right), \quad (10)$$

$$\mathbf{L}_m = [\mathbf{v}, [\mathbf{v}, \mathbf{R}_m - h\mathbf{e}_z]] / v^2. \quad (11)$$

The emitted energy of radiation per unit photon energy and per solid angle is defined by the field of radiation as follows:

$$\frac{dW(\mathbf{n}, \omega)}{d\hbar\omega d\Omega} = \frac{cr^2}{\hbar} |\mathbf{E}(\mathbf{r}, \omega)|^2. \quad (12)$$

Two dispersion relations (2) and (3) were derived from the spectral-angular distribution of SPR (12) (after substitution (8)). They define the condition under which the spectral-angular distribution of SPR is maximal. Both relations were found suggesting that the modified Bessel functions are slowly changed functions of their arguments. This may lead to slight angular or spectral shift of the maximum of SPR from expected values.

4. Angular Distribution

Below there are shown angular dependences of spectral-angular distribution of Smith-Purcell radiation (12) for different values of angle of inclination of the electron trajectory to direction of periodicity χ from 0 to 80 degree for fixed wavelength. The angles of observation are defined as follows:

$$n_x = \cos \theta, \quad n_y = \sin \theta \sin \phi, \quad n_z = \sin \theta \cos \phi. \quad (13)$$

The white dashed lines correspond to two dispersion relations (2) and (3). It is seen that with growing the value of χ the angular patterns becomes more complicated, maxima staying defined by dispersion relations shift. However, the dispersion relations do not define the inclination of the maxima that can be explained by the contribution of the Bessel functions. The particles were supposed to be spherical and their polarizability is defined by function dielectric permittivity ϵ as:

$$\alpha = r_0^3 \frac{\epsilon - 1}{\epsilon + 2}. \quad (14)$$

For all figures $\gamma = 16$, $N = M = 3$, $r_0 = 0.1$ mm, $h = 1$ mm, $d_x = d_y = 2$ mm, $\epsilon = 2$, $\lambda = 1$ mm (0.3 THz).

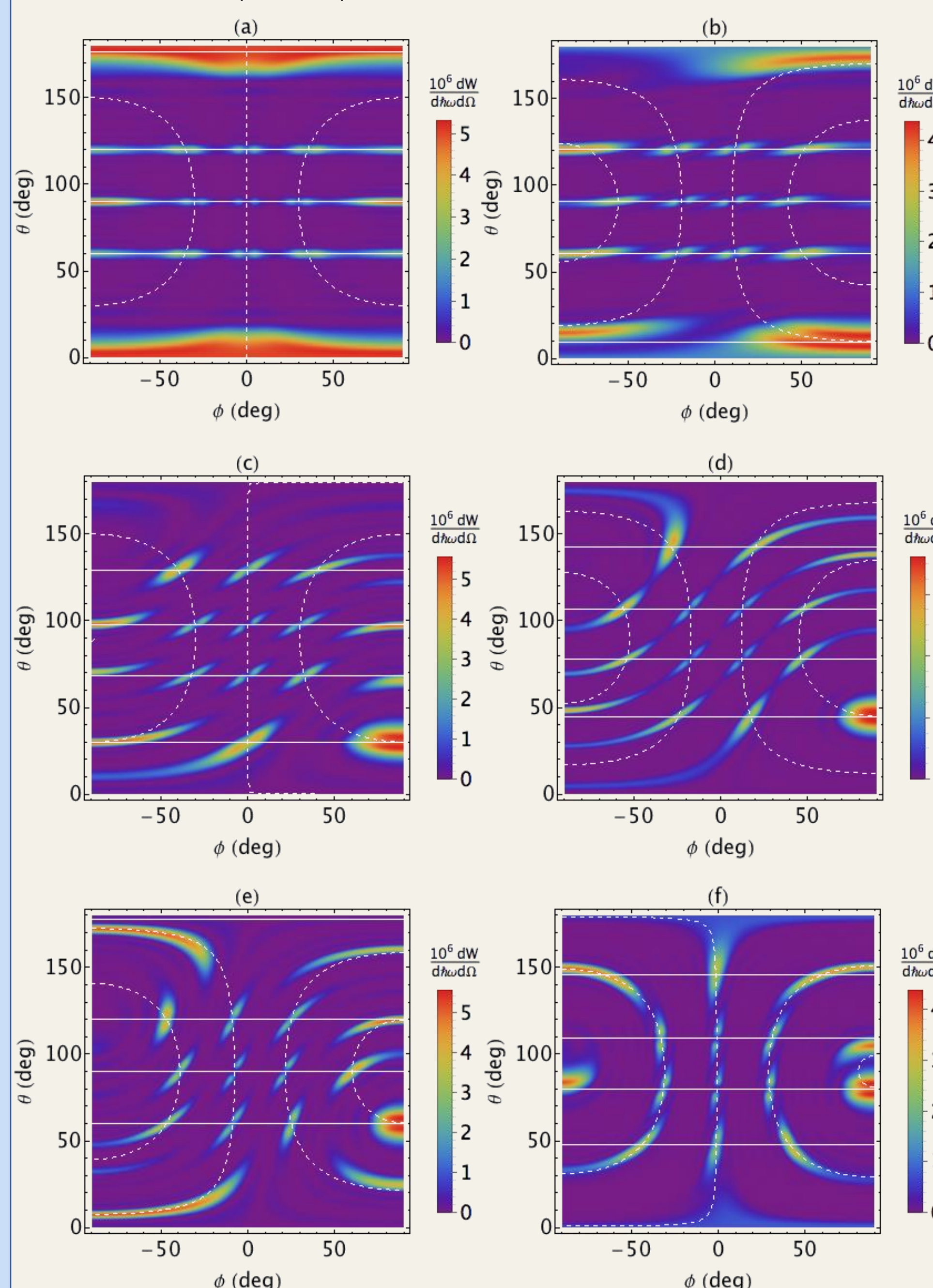


Fig. 3. Spectral-angular distributions of Smith-Purcell radiation for different values of the angle χ : (a) - 0 degree; (b) - 10 degree; (c) - 30 degree; (d) - 45 degree; (e) - 60 degree; (f) - 80 degree.

5. Polarization

Let us consider two components of the electric field (8): one in the plane of radiation (parallel polarization), and another perpendicular to the plane of radiation (perpendicular polarization).

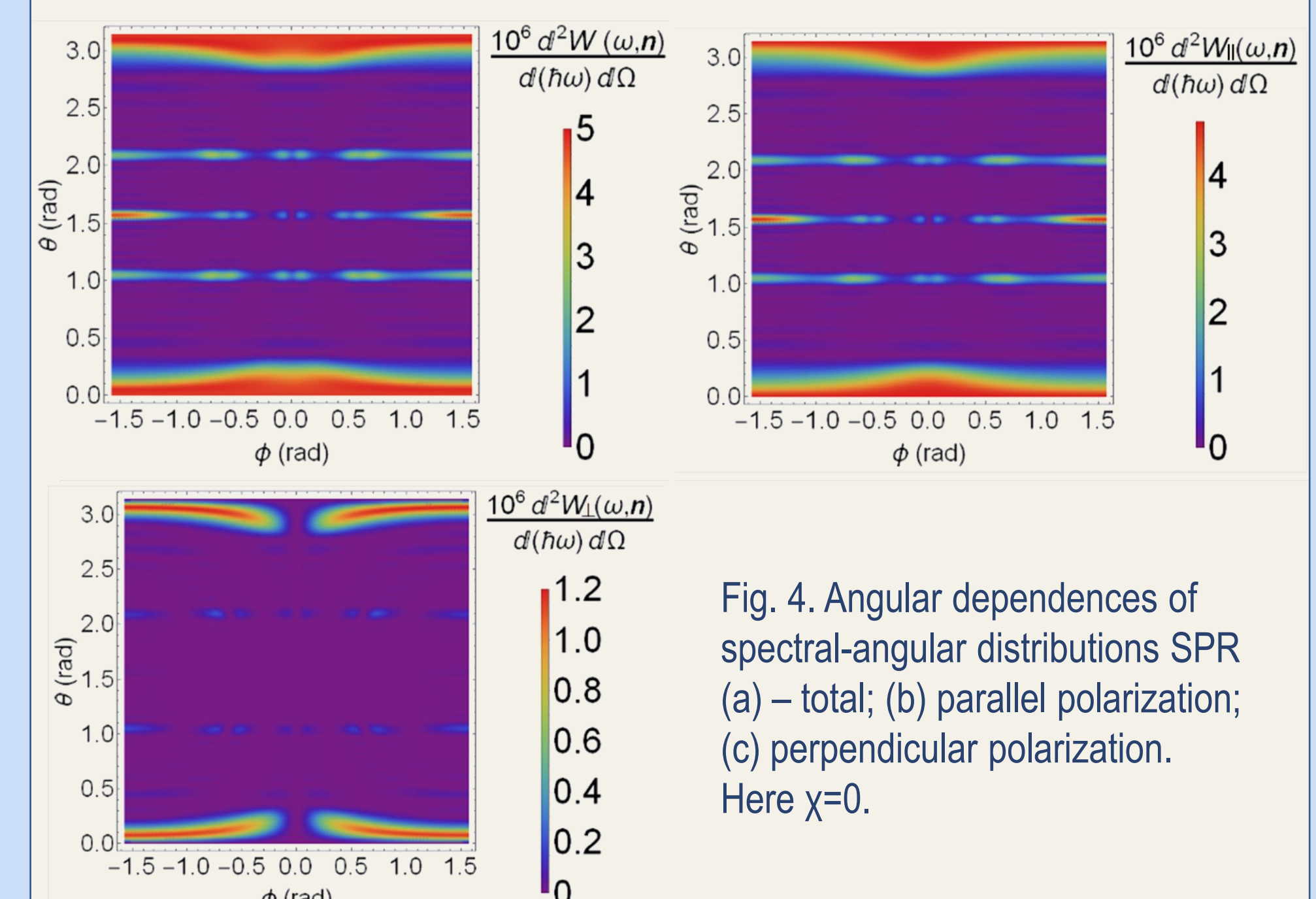


Fig. 4. Angular dependences of spectral-angular distributions SPR (a) - total; (b) parallel polarization; (c) perpendicular polarization. Here $\chi = 0$.

There are two areas with different polarizations: the central part of figures and near $\theta = 0$ and $\theta = \pi$. For the central part the distribution of energy for parallel polarization coincides with the distribution for total energy and it is about 10 times more intense than for perpendicular polarization. SPR from usual gratings is also polarized in the plane of radiation. However, it can be seen that the farther the radiation maxima in angle θ from the value $\pi/2$, the greater the contribution of perpendicular polarization to the total spectral-angular density of radiation. For extreme regions, the magnitude of the highest peak in the graph of perpendicularly polarized radiation is only 4 times less than the maxima in the graph of the total spectral-angular density of radiation, and 3.5 times less than in the graph for parallel polarization. Thus, it cannot be concluded for these extreme regions that this or that radiation polarization is predominant. This conclusion does not depend neither the angle χ or choice of coordinate system (see Fig. 5), nor the target parameters.

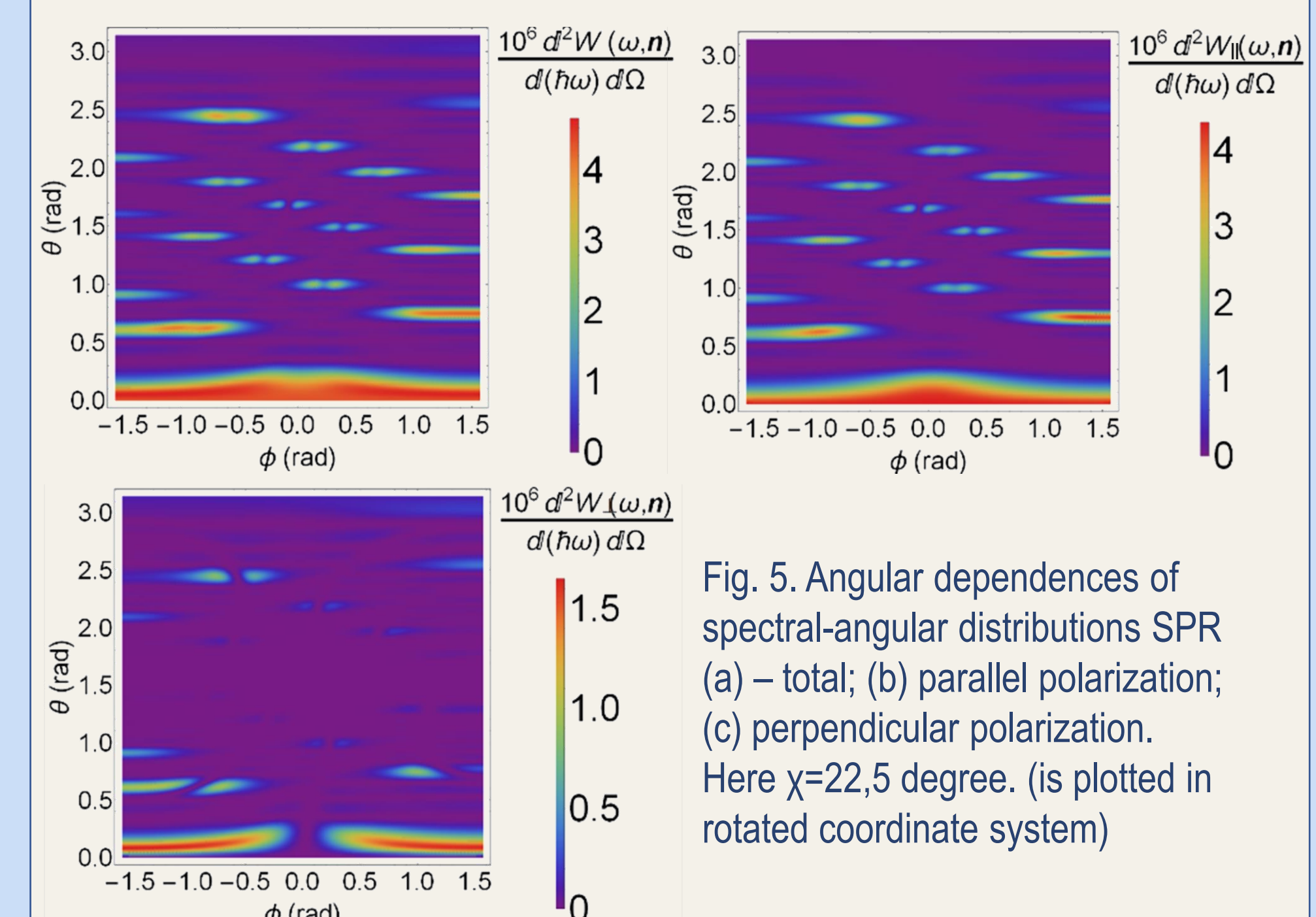


Fig. 5. Angular dependences of spectral-angular distributions SPR (a) - total; (b) parallel polarization; (c) perpendicular polarization. Here $\chi = 22.5$ degree. (is plotted in rotated coordinate system)

6. Conclusion

SPR from the metasurface was studied for an oblique motion of an electron above it. The field and spectral-angular density of the radiated energy were calculated. From the obtained expressions, two dispersion relations were derived that determine the spectral and spatial positions of the radiation maxima. It is shown that when the electron motion deviates from the normal one, the spatial distribution of radiation is significantly complicated, the radiation maxima become much wider in the azimuthal angle.

The characteristic features of SPR from the metasurface differ from an ordinary SPR, firstly, in the appearance of additional maxima outside the plane containing the normal to the surface and the electron trajectory, and secondly, the bifurcation of the maxima. The results can be used to detect the position of the electron beam. Also, the polarization of SPR from the metasurface was investigated. There are areas with different polarization patterns: 1) a narrow region along the electron trajectory, 2) the rest space. In 2) parallel polarization dominates, and perpendicular one is of the order of magnitude less. Both polarizations are dependent on the angle of electron passage. In 1) there is no predominance of one or another polarization. Such a complex picture essentially distinguishes the polarization characteristics of SPR from the metasurface from those of ordinary SPR, which is polarized in the plane of radiation. This can be an additional source of information for diagnosing the position of an electron bunch.



Fig. 6. Photo of an array for generation SPR fabricated in MEPhI Nanocenter

Acknowledgement

This work was supported by the Russian Science Foundation, grant № 19-72-00178.